OsteoArthritis and Cartilage (2007) **15,** 78–89

doi:10.1016/j.joca.2006.06.015

Osteoarthritis and Cartilage

International Cartilage Repair Society

OARSI OSTEOARTHRITIS RESEARCH SOCIETY INTERNATIONAL

Chitosan–glycerol phosphate/blood implants elicit hyaline cartilage repair integrated with porous subchondral bone in microdrilled rabbit defects

C. D. Hoemann Ph.D.†‡*, J. Sun M.D., M.Sc.§, M. D. McKee Ph.D.‖¶, A. Chevrier Ph.D.‡, E. Rossomacha M.D., Ph.D.§, G.-E. Rivard M.D.#, M. Hurtig D.V.M.†† and M. D. Buschmann Ph.D.†‡

† *Department of Chemical Engineering, Ecole Polytechnique, Montreal, QC, Canada*
‡ *Institute of Biomedical Engineering, Ecole Polytechnique, Montreal, QC, Canada*
§ *BioSyntech Inc., Scientific and Hi-Technology Park, Laval, QC, Canada*
‖ *Faculty of Dentistry, McGill University, Montreal, QC, Canada*
¶ *Department of Anatomy and Cell Biology, McGill University, Montreal, QC, Canada*
# *Division of Hematology–Oncology, Hôpital Sainte-Justine, Montreal, QC, Canada*
†† *Comparative Orthopaedic Research Laboratory, Department of Clinical Studies, Ontario Veterinary College, University of Guelph, Guelph, ON, Canada*

Summary

Objective: We have previously shown that microfractured ovine defects are repaired with more hyaline cartilage when the defect is treated with *in situ*-solidified implants of chitosan–glycerol phosphate (chitosan–GP) mixed with autologous whole blood. The objectives of this study were (1) to characterize chitosan–GP/blood clots *in vitro*, and (2) to develop a rabbit marrow stimulation model in order to determine the effects of the chitosan–GP/blood implant and of debridement on the formation of incipient cartilage repair tissue.

Methods: Blood clots were characterized by histology and *in vitro* clot retraction tests. Bilateral 3.5 × 4 mm trochlear defects debrided into the calcified layer were pierced with four microdrill holes and filled with a chitosan–GP/blood implant or allowed to bleed freely as a control. At 1 day post-surgery, initial defects were characterized by histomorphometry ($n = 3$). After 8 weeks of repair, osteochondral repair tissues between or through the drill holes were evaluated by histology, histomorphometry, collagen type II expression, and stereology ($n = 16$).

Results: Chitosan–GP solutions structurally stabilized the blood clots by inhibiting clot retraction. Treatment of drilled defects with chitosan–GP/blood clots led to the formation of a more integrated and hyaline repair tissue above a more porous and vascularized subchondral bone plate compared to drilling alone. Correlation analysis of repair tissue between the drill holes revealed that the absence of calcified cartilage and the presence of a porous subchondral bone plate were predictors of greater repair tissue integration with subchondral bone ($P < 0.005$), and of a higher total O'Driscoll score ($P < 0.005$ and $P < 0.01$, respectively).

Conclusions: Chitosan–GP/blood implants applied in conjunction with drilling, compared to drilling alone, elicited a more hyaline and integrated repair tissue associated with a porous subchondral bone replete with blood vessels. Concomitant regeneration of a vascularized bone plate during cartilage repair could provide progenitors, anabolic factors and nutrients that aid in the formation of hyaline cartilage.

Key words: Cartilage repair, Marrow stimulation, Chitosan, Animal model, Blood clot, Collagen type II, Bone repair, Histomorphometry.

Introduction

Partial thickness cartilage lesions fail to heal and often lead to further degeneration and joint disease[1]. Focal cartilage lesions can be resurfaced in human patients[2–4] and in experimental defects in animals[5–10] when residual cartilage is removed, and access to the vascularized bone marrow provided through abrasion arthroplasty, or debridement and microfracture or drilling[2–4]. However, in both patients[11] and animal models[5–10], the resulting repair tissue is typically fibrocartilaginous or fibrous, tissue types known to have weak biomechanical properties and reduced wear capacity compared to hyaline cartilage, which contains high levels of collagen type II and glycosaminoglycans (GAG)[5,12]. Bone marrow-derived repair cells can give rise to a degree of cartilaginous repair tissue in young rabbits[7,12,13], however, this repair occurs only sporadically in adult rabbits[5–7]. Repair processes, which reliably lead to hyaline cartilage regeneration and integration in skeletally mature defects have yet to be elucidated.

Since bleeding has been identified as an initiating event in post-surgical repair[2–4], we hypothesized that microfracture-based repair could be improved by stabilizing the clot formed in the lesion with a polymer that is thrombogenic and actively stimulates the wound repair process. Chitosan is a positively charged polymer composed of (1 → 4)-β-linked glucosamine and acetyl-glucosamine residues. Previous studies

*Address correspondence and reprint requests to: Caroline D. Hoemann, Ph.D., Department of Chemical Engineering, Ecole Polytechnique, 2900 Chemin Ecole Polytechnique, PO Box 6079, Station Centre-Ville, Montreal, QC, Canada H3C 3A7. Tel: 1-514-340-4848; Fax: 1-514-340-2980; E-mail: caroline.hoemann@polymtl.ca

Received 7 February 2006; revision accepted 25 June 2006.

have shown that chitosan is hemostatic[14–17], and when left in the wound site, stimulates revascularization of the wound[14] and connective tissue repair[14,18–20]. Chitosan is also biodegradable[17,21,22], non-immunogenic[23,24], and adheres to connective tissues including cornea, bone, and cartilage[25,26]. We discovered a means of solubilizing chitosan under physiological conditions by combining it with glycerol phosphate to form chitosan–glycerol phosphate (chitosan–GP) solutions[27–29]. And in a recent study we showed that mixtures of whole blood with chitosan–GP could form solid implants above microfractured cartilage defects[26]. These implants adhered more to the defect than normal clots, and elicited significantly more hyaline repair compared to microfracture alone in an ovine model at 6 months[26].

In the study presented here, we describe the development of a bilateral rabbit cartilage repair model to efficiently screen implants for their ability to improve repair of marrow-stimulated defects as well as to elucidate mechanisms of action. This model was used to test the hypothesis that hyaline cartilage repair after marrow stimulation depends upon the surgical approach and the use of chitosan–GP/blood implants. Chitosan–GP stabilized blood clots were made by combining chitosan–GP solutions with peripheral whole blood from human volunteers, or with blood from two distinct animal species used in cartilage repair studies, rabbit and sheep. Our surgical model was based on a rabbit model previously published by Mitchell and Shepard[6], representing a scaled-down version of human lesions that are treated by microfracture or drilling. This is in contrast to other rabbit models where repair was observed over single, large osteochondral drill holes[13,30,31] which do not mimic human lesions. The generation of rectangular trochlear defects with precisely placed drill holes also permitted us to analyze the effect of treatment on repair tissue formed directly over the drill holes, compared to repair tissue formed over the defect surface between the drill holes.

Methods

MATERIALS

Ultrapure chitosan was obtained from BioSyntech (77.1% degree of deacetylation (DDA), <375 endotoxin units (EU)/g; 79% DDA, <3000 EU/g; 83.4% DDA, <500 EU/g free base from Laval, QC, Canada) or Pronova (84.5% DDA, 130 EU/g, HCl salt from Oslo, Norway). BioSyntech chitosan was dissolved at 1.66% w/v or at 1.89% w/v (taking into account loss on drying) in 60 mM to 83 mM HCl and autoclave-sterilized. Pronova chitosan was lyophilized, weighed, sterilized by exposing the powder to UV light for 90 min, and then dissolved in sterile MilliQ-filtered water at 1.66% w/v, taking into account HCl salt content. Sterile chitosan solutions were combined with filter-sterilized disodium beta-glycerol phosphate (Tissue Culture grade, Sigma, St. Louis, MO) to yield transparent solutions with 1.5% w/v or 1.7% w/v chitosan with 135 mM glycerol phosphate (also called BST-CarGel®), pH 6.8, osmolality of 470 mOsm, and viscosity of 250–1100 mPa s at 25°C, that were stored at −80°C.

BLOOD COLLECTION AND CHITOSAN–GP/BLOOD MIXTURES

All protocols involving animals were approved by institutional animal care committees and all protocols involving human subjects were approved by an Internal Review Board Ethical Committee. Peripheral whole blood was collected aseptically from the central ear artery from 15 New Zealand White rabbits with atravet or ketamine/xylazine/buprenorphine and isoflurane gas anesthesia and the jugular vein of 10 sheep with or without ketamine/diazepam and halothane gas anesthesia. Anesthetics can affect platelet function[32], however, whole blood clotting times from anesthetized animals and unanesthetized humans were similar to published values[33]. Venous blood was collected aseptically from non-fasting healthy volunteers ($n=7$, 23–43 years old). Non-activated whole blood was drawn into plastic syringes after a 2 mL first discard, with a 21-gauge 3/4 inch butterfly needle with female luer and outlet needle. Homogeneous aseptic mixtures were obtained by filling 4.0 mL Wheaton glass vials with plastic screw-caps to capacity with 1.1 mL chitosan–GP solution, 3.3 mL fresh blood, and six surgical 316 stainless steel mixing beads (4.5 mm diameter, Salem Specialty, Canton, CT), closing the vials, and shaking vigorously for 10 s.

BLOOD SMEARS, CLOTTING TIME, CLOT RETRACTION, AND HEMOLYSIS MEASUREMENTS

Blood smears were generated with blood or chitosan–GP/blood mixtures within 3 min after mixing and stained with May Grunwald Geimsa (Sigma, St. Louis, MO). Clotting time was measured using the Lee–White clotting test in dry, sterile, non-siliconized glass tubes with vented steel caps and 0.5 mL sample volumes[34]. Tubes containing 0.5 mL solid clot samples were transferred to a humidified 37°C incubator for 4 h to determine percent retraction by weighing separately the excluded serum and mass of the solid clot. Hemolysis was determined by serum hemoglobin absorbance at OD_{530} using an enzyme-linked immunosorbent assay (ELISA) plate reader, modified from a previous method[35].

FEASIBILITY STUDIES

To test the effect of removal of the calcified cartilage layer on repair with or without implant, bilateral defects were created identically in each trochlear groove in the knees of skeletally mature rabbits. In three rabbits, defects were debrided into, but not beyond, the calcified cartilage while in another three rabbits, bilateral defects were completely debrided of the calcified layer to bleeding cancellous bone. All defects were then pierced with four or five, 0.9 mm diameter 3 mm deep holes with either a drill bit or a custom-made pick and hammer. Chitosan–GP/blood implant was solidified in one defect while the contralateral defect was allowed to bleed as a surgical control. Defects were allowed to repair for 7–11 weeks then fixed, decalcified, processed in LR White plastic resin, stained with Toluidine Blue and analyzed histologically.

RABBIT CARTILAGE REPAIR MODEL

Thirty-eight bilateral defects were created in the knees of 19 skeletally mature New Zealand White rabbits (9–15 month old females, 4.6 ± 0.8 kg, Table I). Three of these rabbits were used to evaluate the initially debrided defects at 1 day post-op while defects in the remaining 16 rabbits were evaluated at 8 weeks post-op. Rabbits were anesthetized by an intramuscular injection of ketamine/xylazine/buprenorphine, and maintained on 3% isoflurane/oxygen. The ears (phlebotomy site) and legs were shaved and disinfected with Baxedin, poviodine, and 70% ethanol.

Table I
Rabbit cartilage repair study design

Number of animals	Treated defects	Control defects	Repair period
$N = 3$	$N = 3$ (right knee)	$N = 3$ (left knee)	1 day
$N = 16$	$N = 8$ (right knee) $N = 8$ (left knee)	$N = 8$ (left knee) $N = 8$ (right knee)	8 weeks

Cartilage defects were created in each trochlear groove using sequential bilateral arthrotomies with a medial parapatellar incision followed by patellar luxation. Joint surfaces were kept moist with sterile phosphate buffered saline (PBS) irrigation every 30–60 s to maintain viability of cells in the exposed articular and calcified cartilages. Chondral defects (3.5 × 4 mm) were made in the center of the trochlear groove to a depth of around 200 μm, 3–5 mm above the lateral collateral ligament insertion, by scraping with 1.5–2.75 mm flat surgical blades (Fine Science Tools, North Vancouver, B.C., Canada) into the calcified cartilage. Four, 3–4 mm deep microdrill holes were then generated in each of the corners of the defect using a high-speed, handheld microdrill and 0.9 mm diameter drill bit (Fine Science Tools, North Vancouver, B.C., Canada) with constant 4°C PBS irrigation to avoid thermal necrosis and to wash away bone debris. Bleeding from subchondral holes, which was minimal in >10 month old rabbits, was additionally promoted by inserting a 26-gauge 1/2 inch needle into each hole. Once the defects were hemostatic, freshly drawn whole blood was mixed with chitosan–GP (79% DDA chitosan), drawn into a 1 cc syringe with a 20-gauge needle, and one drop (~25 μL) deposited directly onto the horizontally held defect within 2 min of mixing where the implant solidified within 7–9 min. These ~25 μL implants were larger than the 3.5 × 4 × 0.2 mm chondral defect volume (~2.8 μL), and completely covered the defect. Defects were treated with chitosan–GP/blood in alternating right and left knees (Table I). Contralateral defects were allowed to fill with bone-derived blood without further intervention, as in standard drilling procedures[2] and served as controls. The patella was repositioned and the knee closed in sutured layers. Animals were allowed immediate unrestrained activity in cages after recovery from anesthesia, and received buprenorphine anti-pain medication twice daily for 3 days following arthrotomy. No antibiotics were given. All joints at sacrifice were free from infection, and at necropsy rabbits had neither effusions nor weight loss. Eight out of the 16 rabbits were housed in free-range enclosures (2.6 × 2.7 m) prior to surgery and for the final 4–6 weeks of the 8 week repair period while all other rabbits were housed in cages (0.6 × 0.6 × 0.4 m, length–width–height) for the entire repair period.

HISTOPROCESSING AND IMMUNOHISTOCHEMISTRY

All clot samples were fixed after 1–4 h post-solidification in 4% glutaraldehyde/PBS or 10% buffered formalin and then either processed in LR White plastic resin and stained with Toluidine Blue, or processed in paraffin and stained with Safranin O/Fast Green/Iron Hematoxylin to identify chitosan by specific Fast Green-specific staining characteristics[36]. Immediately after sacrifice, distal femora were recovered, dissected of all soft tissues and fixed for 3 days in 4% paraformaldehyde/1% glutaraldehyde/100 mM sodium cacodylate, pH 7.2. Defects from 1 day post-op were decalcified in ethylenediaminetetraacetic acid (EDTA), and cryosections generated from the middle of each defect and stained with Safranin O/Fast Green. Defects after 8 weeks of repair were decalcified in 0.5 M HCl/0.1% glutaraldehyde for 7–10 days then trimmed and bisected transversely with a razor between the drill holes. The proximal defect half was embedded in LR White plastic resin, while the distal half was embedded in paraffin. Five to 20, 1 μm-thick plastic sections were generated in the proximal half of the repaired defects, including between the drill holes, within the drill holes, and proximal to the drill holes and stained with Toluidine Blue. Paraffin sections 6 μm thick were generated from the distal half within the drill holes, then dewaxed, digested with 2.5% w/v hyaluronidase and processed by immunohistochemistry as previously described[37] for collagen type II using monoclonal II-II6B3 (DSHB, Iowa, USA) at 1:10 dilution, biotinylated goat anti-mouse diluted to 22 μg/mL, and avidin-Alkaline Phosphatase-red substrate detection (Vector Laboratories Inc., Burlington, Ontario, Canada), followed by light Iron Hematoxylin counterstain. Control isotype antibody or omission of primary antibody showed no staining.

QUALITATIVE HISTOLOGICAL SCORING AND QUANTITATIVE HISTOMORPHOMETRY

Four to 12 sections from distinct areas within the proximal half of each defect were graded by a blinded observer using the O'Driscoll score[31], with the exception that staining intensity was determined with Toluidine Blue instead of Alcian Blue. The score for normal cartilage is 24[31]. This evaluation revealed that the edge of the "tufts" of repair tissue covering the drill holes contained less differentiated cells than the center of the tufts, as previously reported by Mitchell and Shepard[6]. Therefore, one section in the middle of the holes and one section between the holes were selected from each defect to compare O'Driscoll scores. All histomorphometric and stereologic analyses were performed on these same two plastic-embedded sections by a blinded observer, using a Zeiss Axiovert microscope, digital camera, and histomorphometric software (Northern Eclipse, Empix Imaging, Mississauga, ON) to measure the width of the cross-section of each defect, the percent of different tissues covering the defect (repair tissue, bone or calcified cartilage), and the percent of repair tissue clearly detached from the base of the defect. The same histomorphometric analysis for percent of different tissues covering the initial defects was performed on one section from the middle of each defect after 1 day of repair ($n = 3$ sections per condition). In sections from defects repaired for 8 weeks, percent of integrated repair tissue was determined as the total length of the repair tissue attached to the defect base divided by the defect width. Repair tissue area was determined as the cross-sectional area of tissues above subchondral bone, excluding bone, and excluding soft tissues occasionally present in the drill holes. Collagen type II staining in repair tissue above the subchondral bone was quantified by threshold analysis as the percent of total repair tissue area that stained pink and light red, vs a dark red hue that matched the staining intensity of normal cartilage[37].

For stereology measurements, digital print-outs were generated of a segment of subchondral bone directly beneath the repair tissue (250 μm deep, the entire width of the defect) to measure bone porosity. Histologically identified pores were traced with a line tool to render them more visible. A grid with 19.75 μm × 19.75 μm squares was randomly positioned over the sample image and the number of intersections (I) of grid lines with the surfaces

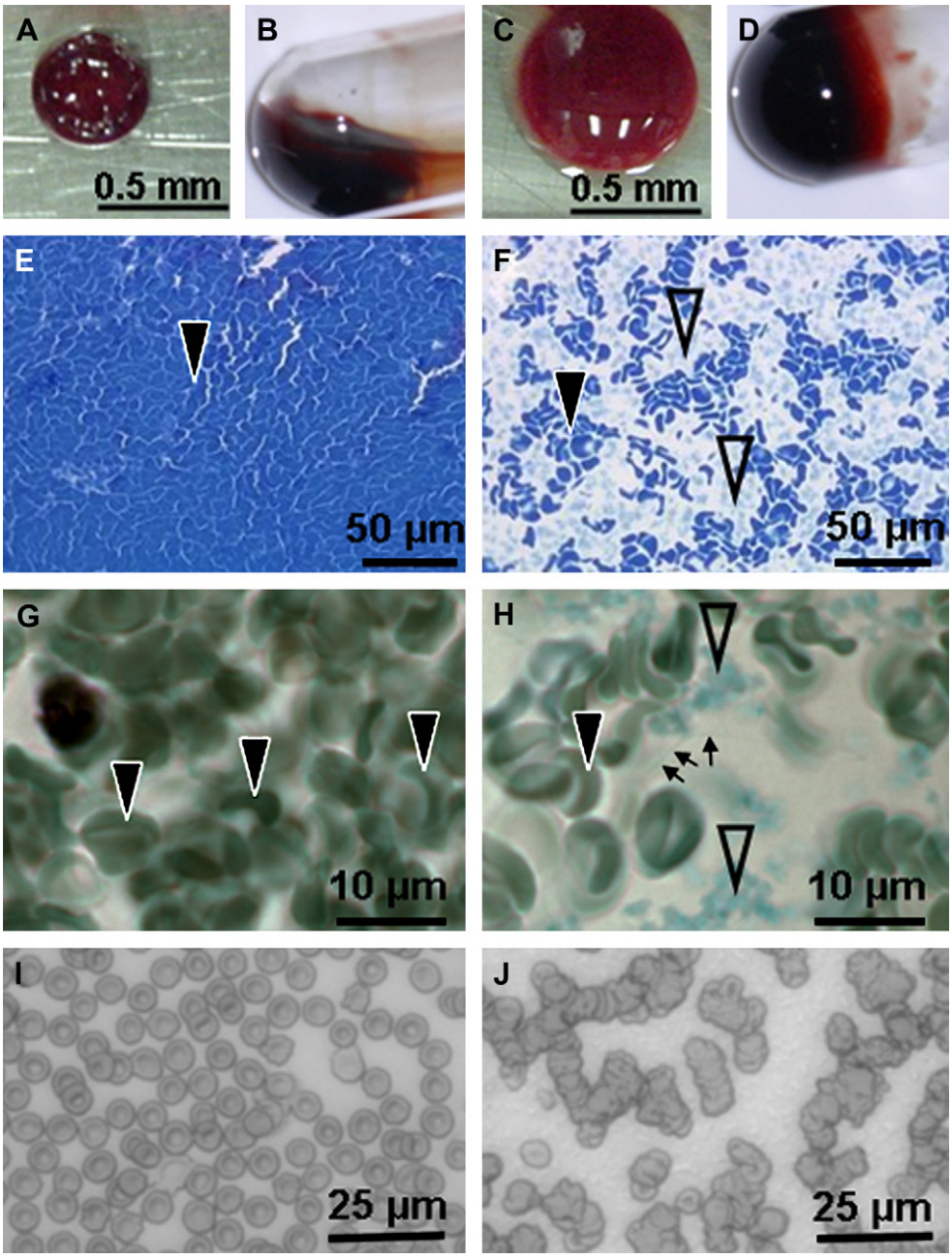

Fig. 1. Chitosan–GP/blood mixtures generate clots that resist retraction, contain fibrin-like fibers and RBC aggregates. Sample clots (0.5 mL) were cultured at 37°C for 1–4 h in glass culture tubes. Whole blood clots retracted (A and B), while chitosan–GP/blood clots retracted very little (C and D). Histology of clot samples in plastic (E and F), or paraffin (G and H) showed biconcave RBCs (black arrowheads) with fibrin-like fibers (H, black arrows) and light blue or Fast Green-stained chitosan[36] (open arrowhead) dispersed homogeneously among clumps of RBCs. Blood smears showed chitosan-specific erythrocyte aggregates (J) compared to normal blood (I), which were not detected in GP/blood mixtures (data not shown). Samples were generated with sheep (A and C), human (B, D, G and H) or rabbit whole blood (E, F, I and J).

of all pores was manually counted. In addition, we counted the number of points (grid intersections) that fell within all bone pores (P) and within the entire bone sample (B), the latter serving as a reference volume[38]. Pore surface area per reference volume (Sv in $\mu m^2/\mu m^3$) was calculated according to the equation $Sv = I/(B \times 0.01975\ mm)$[38]. Pore volume per reference volume (Vv, in percent m^3/m^3) was obtained according to the equation $Vv = P/B$[38]. Some degree of sampling bias was present in these measurements, due to the unavoidable anisotropy and non-random orientation of the osteochondral sections.

STATISTICAL ANALYSIS

To test the hypothesis that treatment affected repair, differences in O'Driscoll histological scores were analyzed by the Mann–Whitney U test for one section per defect over the holes ($n = 16$) and one section per defect between the

holes ($n = 16$) (Statistica version 6.1, Tulsa, OK). Differences were considered significant for P exact values, $P < 0.05$. The Student's t test was used to determine whether clot retraction was significantly different between chitosan–GP and normal blood clots 4 h post-solidification, and whether chitosan–GP/blood implants significantly improved histomorphometric and stereological variables compared to blood clots alone. Correlation coefficients were obtained by multivariate analysis of covariate scatterplots (Statistica version 6.1, Tulsa, OK) with significance determined when $P < 0.05$.

Results

CHITOSAN–GP SOLUTIONS STABILIZE BLOOD CLOTS

Mixing experiments were performed in order to create hybrid chitosan blood clots that solidified within 10 min. Trials with different ratios of blood and chitosan–GP solutions revealed that homogeneous chitosan–GP/blood clots formed most rapidly using a ratio of 1 volume chitosan–GP to 3 volumes whole blood from rabbit, sheep, or human. After 1 h at 37°C, whole blood clots retracted up to 40% of their original mass, were stiff and non-elastic [Fig. 1(A,B)]. In contrast, hybrid chitosan–GP/blood clots containing final concentrations of 0.4% w/v chitosan and 34 mM glycerol phosphate were firm and elastic [Fig. 1(C,D)]. Mixture of chitosan without glycerol phosphate (pH 4.7) into whole blood resulted in unstable and brittle clots with substantial hemolysis that was not seen in normal clots or in chitosan–GP/blood clots (data not shown). Compared to normal clots [Fig. 1(E,G)], chitosan–GP/blood clots were comprised of a chitosan scaffold homogeneously dispersed among clumps of red blood cells (RBCs) with histologically visible fibrin-like fibers [Fig. 1(F,H)]. In blood smears generated from fresh chitosan–GP/blood mixtures, chitosan specifically mediated adhesion between RBCs (Fig. 1, compare panels I and J). Chitosan–GP/blood clots retracted significantly less than the normal clots [Fig. 1(A–D)] in three different species ($P < 0.0001$, Fig. 2).

EFFECT OF SURGICAL DEBRIDEMENT ON CARTILAGE REPAIR

In skeletally mature rabbits, the trochlear calcified cartilage layer had an average thickness of 77 ± 20 μm, sometimes attaining half the thickness of the non-mineralized articular cartilage, which in the area of the defects had an average thickness of 160 μm ± 41 μm ($n = 6$). A preliminary study was performed to examine the effect of debridement of the calcified layer on cartilage repair. Complete debridement of the calcified layer to the bleeding cancellous bone followed by marrow stimulation led to severe subchondral bone resorption and fibrous repair [Fig. 3(A,C,E)]. By comparison, defects that were debrided into the calcified layer, drilled, and treated with chitosan–GP/blood implant developed variable amounts of hyaline repair tissue [Fig. 3(B,D,F)]. Based on these results, our study was conducted using drilled defects that had been debrided into, but not beyond, the calcified layer [Fig. 4(A)]. Control defects were allowed to fill with bone-derived blood [Fig. 4(A), inset], while treated defects were filled with chitosan–GP/blood which formed a solid implant after 7–10 min [Fig. 4(B), Table I]. Histomorphometry of initial defects showed that an average 40% of the cross-section of the defect between the drill holes was covered by residual calcified cartilage, the remainder of the defect consisting of exposed subchondral bone [$n = 3$, Fig. 5(A)].

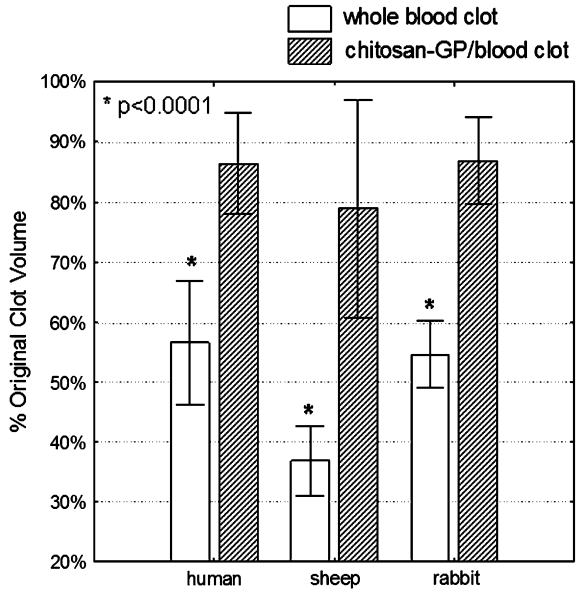

Fig. 2. Chitosan–GP incorporation into blood significantly inhibits clot retraction. Chitosan–GP/blood clots retained more volume ($P < 0.0001$) after 4 h at 37°C using whole blood from human ($n = 7$), sheep ($n = 10$), and rabbit ($n = 9$).

EFFECT OF THE CALCIFIED LAYER AND CHITOSAN–GP/BLOOD IMPLANTS ON BONE REPAIR, AND THE INTEGRATION AND QUALITY OF CARTILAGE REPAIR

After 8 weeks of repair, an animal-specific, bilaterally consistent macroscopic filling was seen in the trochlear defects. In 11 rabbits, bilateral defects were covered with tufts of repair tissue over the drill holes [Fig. 4(C,D)], while in five rabbits, both defects were completely resurfaced [Fig. 4(E,F)]. Control repair tissue was typically white and streaky while treated repair tissue was white and glassy. Histological sections taken between the drill holes showed that defects with tufts of repair tissue had persistent calcified cartilage [Fig. 6(A–D)]. In some rabbits, the control defect between the drill holes was completely devoid of repair tissue [Fig. 6(A,C)], while the contralateral treated defect contained tufts of hyaline repair tissue growing above porous bone and breaching the calcified layer [Fig. 6(B,D)].

Histomorphometry of the tissues covering the defects after 8 weeks of repair revealed that less average calcified cartilage was present compared to the initial defects, with correspondingly less calcified cartilage remaining in treated defects both between and through the drill holes [Fig. 5(A)]. A similar average volume of repair tissue covered the control and treated defects [Fig. 5(B)]. However, in many control defects, the repair tissue was growing from the drill holes and over, but not integrating with, the defect base [Figs. 6(E,G), 7(A,B)]. An average 12% of repair tissue covering the control defects between the drill holes was detached from the base of the defect, while only 1% of repair tissue covering treated defects was detached [$P < 0.05$, Fig. 5(C)]. Treated defects were resurfaced with more integrated repair tissue between the drill holes [76% treated vs 39% control, $P < 0.005$, Fig. 5(C)]. After 8 weeks of repair, repair tissues in many defects had not yet reached the edges of the defect, giving a median score of 0 for bonding with the adjacent cartilage

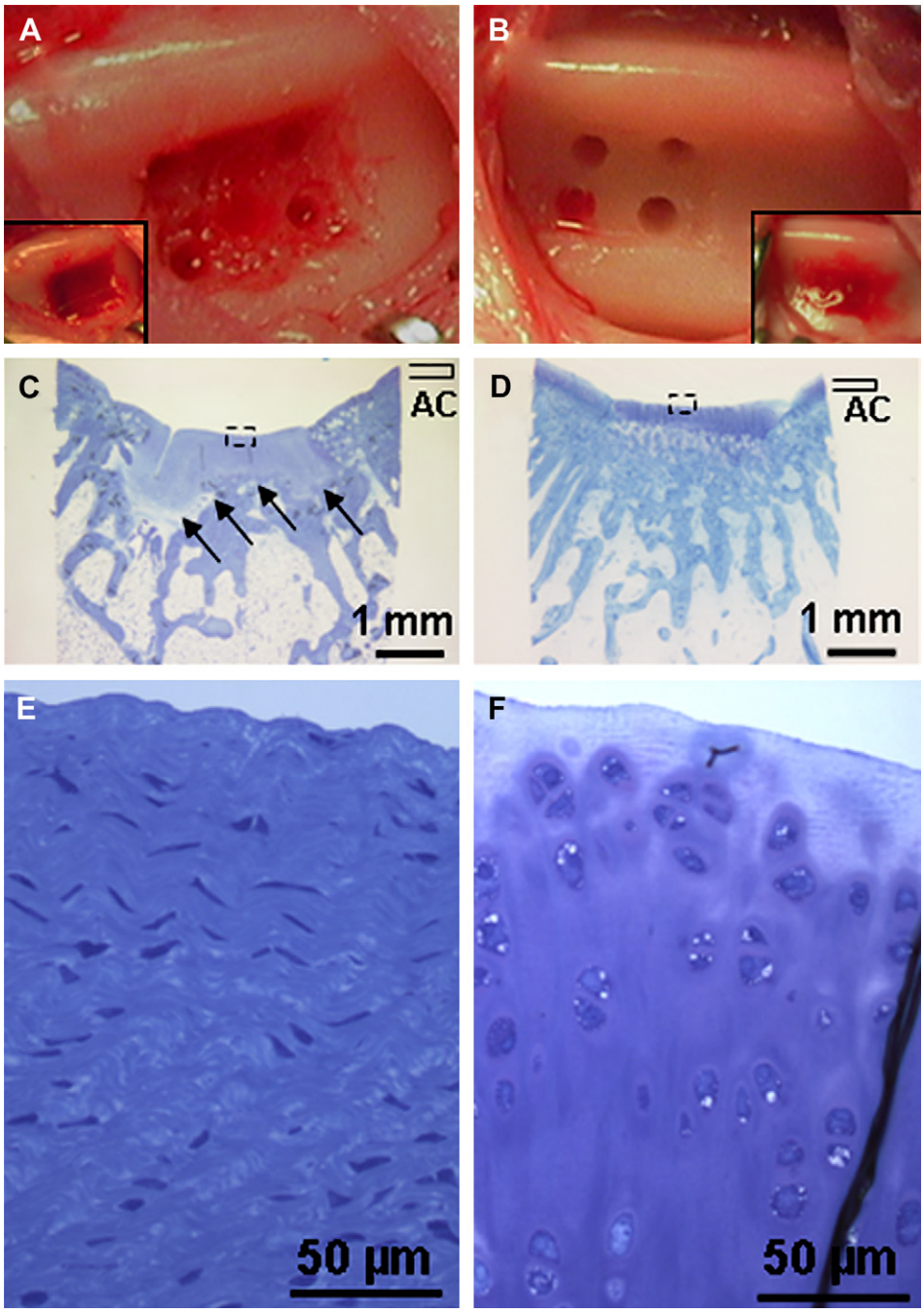

Fig. 3. Development of fibrous or hyaline repair following marrow stimulation depends on the extent of debridement. Bilateral trochlear defects were generated in the knees of skeletally mature rabbits by debriding the calcified cartilage layer completely and administering five microfracture holes (A) or by debriding into the calcified cartilage layer and piercing four microdrill holes (B). In each rabbit, one defect was allowed to fill with bone marrow-derived blood (for example, A, inset), while the contralateral defect was filled with chitosan–GP/blood which was allowed to clot *in situ* (for example, B, inset). Repair at 7–11 weeks showed that defects debrided of the calcified layer had extensive subchondral bone resorption and fibrous tissue repair (C and E), while more hyaline repair was seen in defects debrided slightly into the mineralized zone with no visible punctuate bleeding that were then drilled, and treated with chitosan–GP/blood implant (D and F). Arrows: resorbed bone. AC: articular cartilage layer.

[Fig. 6(A,B,E,F); Table II, parameter VI]. Treatment led to repair tissue with more intense staining for collagen type II over the drill holes [$P < 0.005$, Figs. 5(D), 7]. Treatment also led to greater hyaline cartilage morphology, Toluidine Blue staining intensity, slightly more cellularity, and higher total O'Driscoll scores (P values: $P < 0.05$ to $P < 0.0005$, Table II). More remarkable histological differences between treated and control repair tissues were observed between the drill holes and these differences are summarized in Table II.

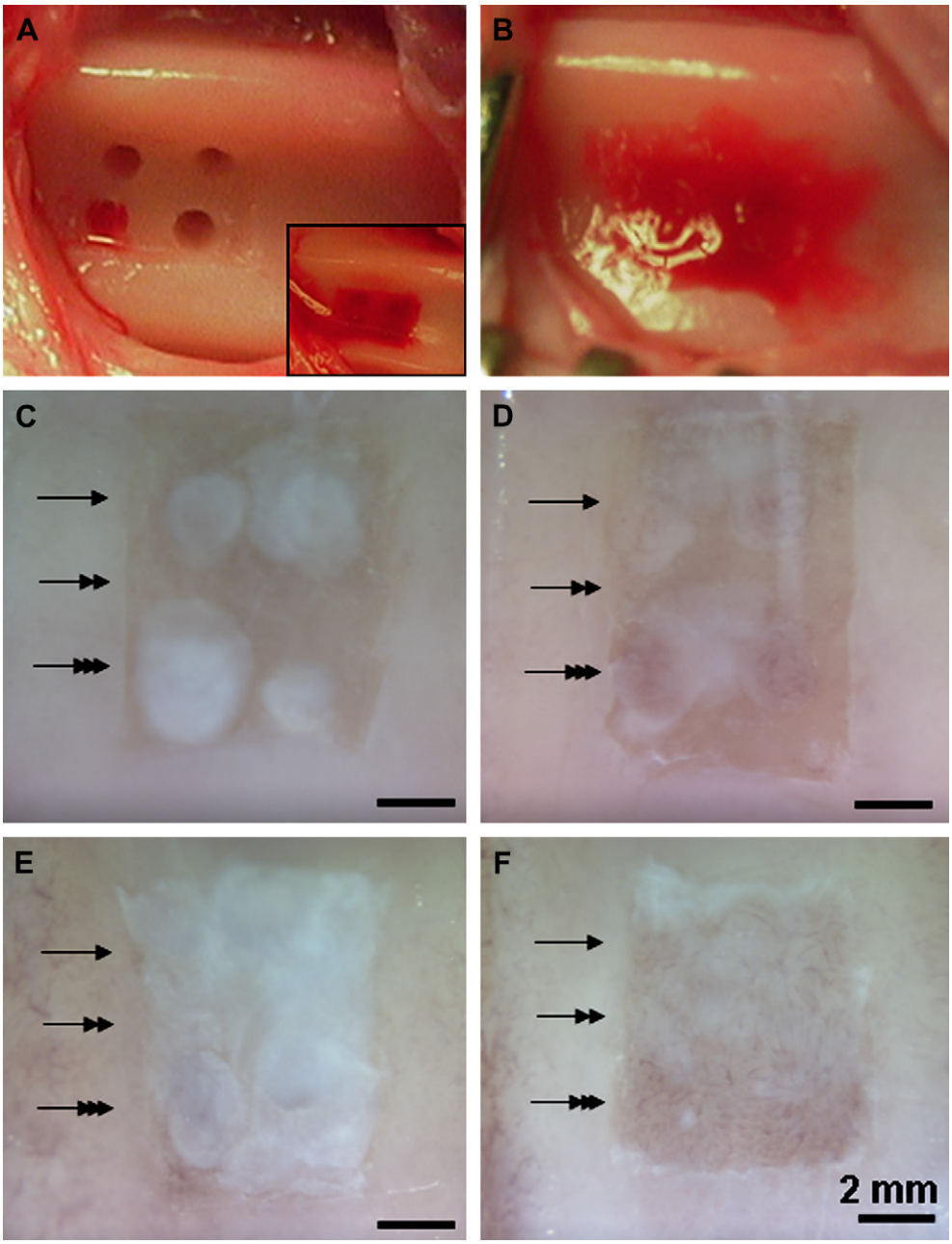

Fig. 4. Appearance of defects and implant at surgery, and bilateral repair at 8 weeks post-surgery. All defects were debrided into the calcified layer with four drill holes (A) and allowed to bleed as a control (inset of A, C, and E) or treated with chitosan–GP/blood implant (B, D, and F). Two patterns of repair were observed where bilateral defects either had tufts of tissue growing from the drill holes in 11 out of 16 rabbits (C and D) or were completely resurfaced in five out of 16 rabbits (E and F). Treated defects had a distinct macroscopic appearance compared to surgery-only controls. The single and double arrows indicate the areas used to generate plastic Toluidine Blue-stained sections through and between the drill holes for histomorphometric, histological, and stereological analyses. The triple arrow indicates the region where paraffin sections were generated for collagen type II immunostaining over the distal holes.

TREATMENT ELICITED HYALINE REPAIR THROUGH A MECHANISM INVOLVING BONE REPAIR AND REMODELING

Hyaline repair was frequently associated with porous, vascularized subchondral bone [Fig. 6(D,H), open arrows; Fig. 7(E), dotted black circles]. In the superficial 250 μm of the repaired subchondral bone plate, treatment was found to increase the pore surface area (Sv) and pore volume (Vv) over the holes [$P < 0.005$, Fig. 5(E,F)]. This effect was partly due to the fact that in many controls, the microdrill holes had repaired with fibrous tissue instead of bone [Fig. 7(B)]. A lack of bone repair at 8 weeks in the microdrill holes was associated with fibrous or fibrocartilage repair [Fig. 7(C)]. Treatment also increased Sv and Vv between the holes ($P < 0.005$), consistent with the observation that treatment elicited remodeling of the subchondral bone plate between the drill holes at earlier time points, between 2 and 5 weeks post-surgery[39]. Sv correlated positively with Vv for all 32 defects ($P < 0.0001$), approximately doubling in

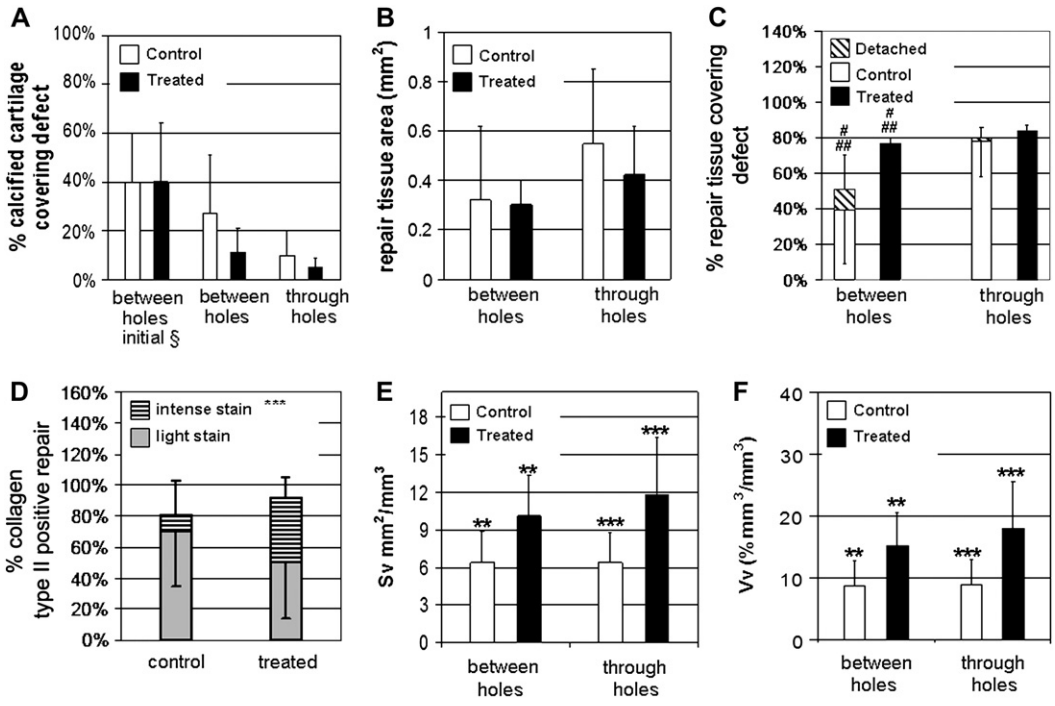

Fig. 5. Histomorphometric and stereological analyses. Initial defects repaired for 1 day ($\S n = 3$) were analyzed only for residual calcified cartilage (A) while defects repaired for 8 weeks ($n = 16$) were submitted to all of the analyses (A–F). All data are given as the average ± standard deviation. (A) Percent of defect width covered by residual calcified cartilage was quantified between the drill holes of initial defects, and between or through the drill holes of 8 week repaired defects. (B) Cross-sectional repair tissue area over and between the holes. (C) Percent of repair tissue covering the cross-sectional area of the defect that was integrated (white and black bars) or detached (hatched bars) from the base of the defect. (D) Percent collagen type II staining tissue (light staining, grey or black bars; intense staining, striped bars) detected in the total repair tissue area over the distal drill holes. Stereological analysis of the superficial 250 μm region of the subchondral bone plate for (E) bone pore surface area per reference volume (Sv), or (F) bone pore volume per reference volume (Vv). Symbols: § = samples from day 1 post-operative; $^{*}P < 0.05$, $^{**}P < 0.005$, and $^{***}P < 0.0005$, compared to control; $\#P < 0.05$ for detached repair tissue compared to treated, and $\#\#P < 0.005$ for integrated repair tissue compared to control.

both cases, thereby maintaining a similar pore volume to surface area ratio. These data suggest that gross pore morphology was not altered by treatment, but rather that the pore number was increased by treatment throughout the bone immediately below the defect. The average Sv of the subchondral bone plate below control vs treated defects [6 vs 10 mm^2/mm^3, Fig. 5(E)] was in-between Sv values previously obtained for cortical bone vs cancellous bone (2.5 vs 20 mm^2/mm^3)[40].

A covariate correlation analysis of all defects ($n = 32$) revealed that the absence of calcified cartilage was a significant predictor of integration of repair tissue with the

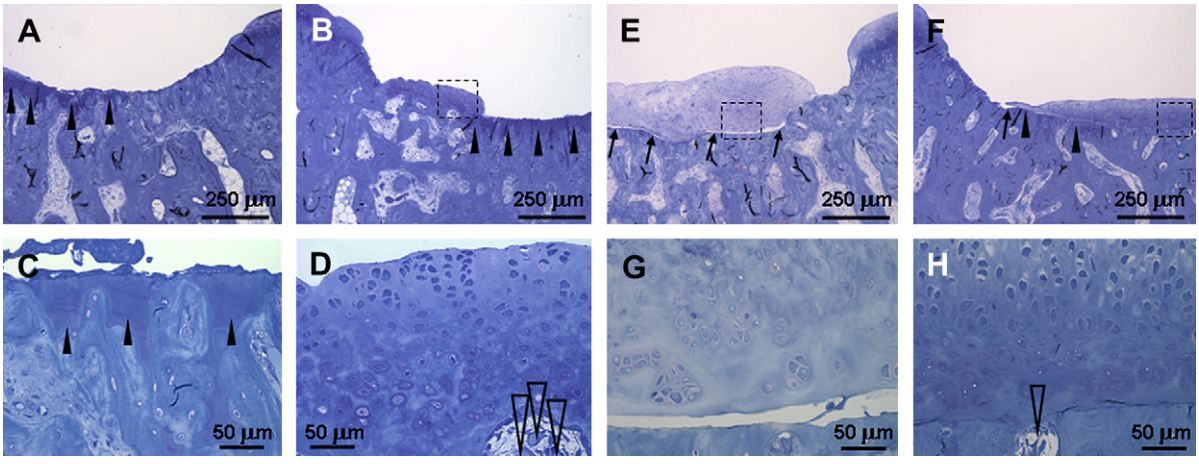

Fig. 6. Histology of Toluidine Blue-stained plastic sections taken from between the drill holes of bilateral defects at 8 weeks. Control defects (A, C, E, and G) and contralateral treated defects (B, D, F, and H) are shown for the bilateral defects with tufts of repair tissue shown in Fig. 4(C,D) (panels A through D), or the completely resurfaced bilateral defects from Fig. 4(E,F) (panels E through F). Hyaline repair was defined according to O'Driscoll[31] as a repair tissue containing cells with a chondrocyte morphology surrounded by distinct lacunae, and more intense Toluidine Blue staining. Subchondral bone pores associated with hyaline repair (D and H) contained blood vessels (open arrowheads).

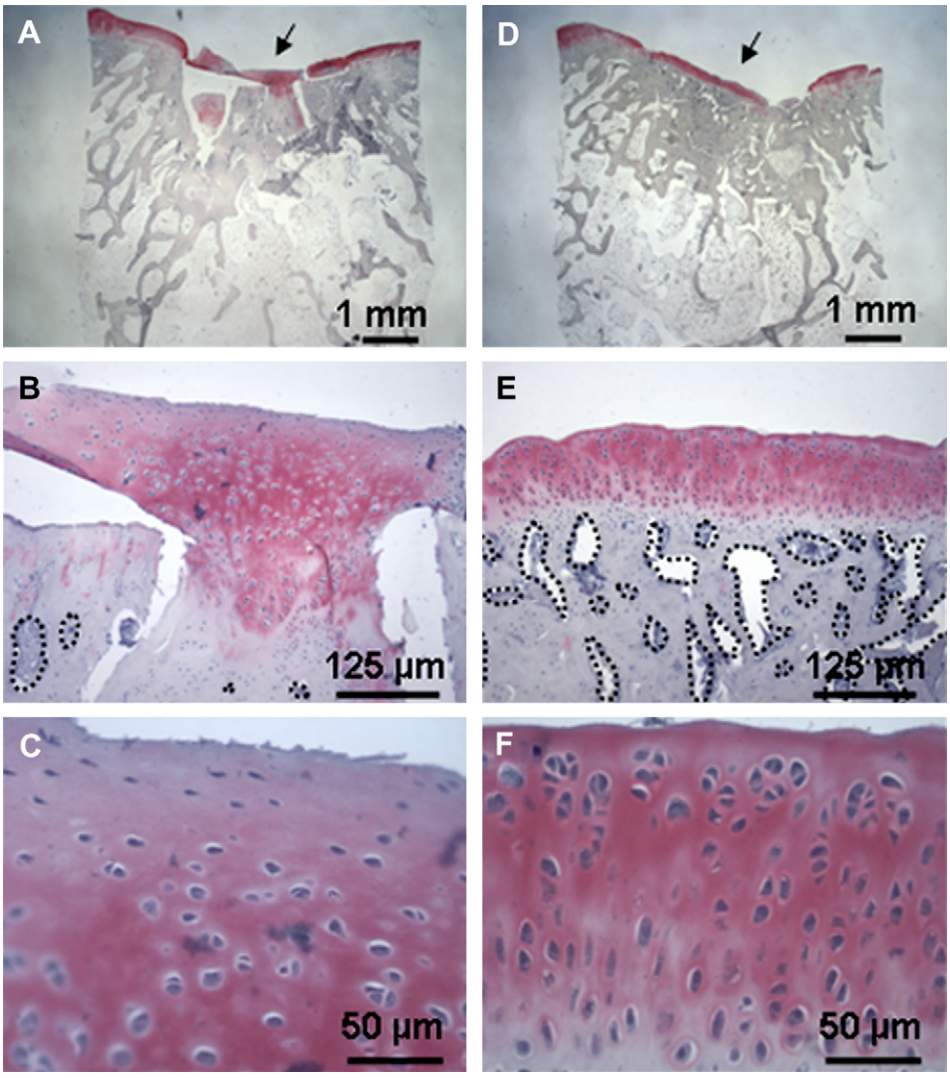

Fig. 7. Chitosan–GP/blood implants create a repair tissue at 8 weeks that is more integrated, with more intense collagen type II expression over porous bone. Immunohistochemistry for collagen type II is shown for repaired bilateral defects from a rabbit where the defect was completely resurfaced. Repair over former drill hole is indicated for respective defects (black arrows, upper panels), and the region under the arrow shown at successively higher magnifications directly below. In this representative control defect (A, B, and C), the drill holes had incomplete bone repair, with a fibrocartilage tissue growing over the defect which failed to attach to the bone, with somewhat lighter superficial collagen type II stain and a non-porous subchondral bone plate (A, C, and E). The contralateral chitosan–GP/blood treated defect had a homogeneous complete repair of the drill holes with porous bone (dotted black circles, E), complete tissue integration (A and E), and a more hyaline appearance with columnar cell organization and higher cell density (F).

subchondral bone both over ($P < 0.005$) and between microdrill holes ($P < 0.01$). Other predictive relationships between variables were only observed between the drill holes and not over the drill holes. Between drill holes, the absence of calcified cartilage predicted a higher total O'Driscoll score ($P < 0.005$), while a higher bone pore surface area (Sv) in the subchondral plate was a predictor of better repair tissue integration ($P < 0.005$), and a higher total O'Driscoll score ($P < 0.01$).

Discussion

CLOT STABILIZATION BY CYTOCOMPATIBLE CHITOSAN SOLUTIONS

Chitosan–GP/blood clots are novel implants with wound-healing properties originating both from whole blood components, and the chitosan itself. Acidic chitosan solutions and solid chitosan substrates have been previously shown to be pro-coagulatory[14], by generating a RBC thrombus[16], and by promoting platelet aggregation and degranulation[15–17,41–43]. Our data now extend these observations to show that liquid mixtures of whole blood and chitosan–GP can generate solid, homogeneous polymer-reinforced hybrid clots. Chitosan–GP solutions mediated erythrocyte–erythrocyte adhesion, suggesting that the surgically implanted chitosan–GP/blood clot implants had greater bonding between RBCs than normal clots. The available data[41,44] suggest that platelets are activated in the hybrid chitosan–GP/blood clots, but are somehow inhibited from fully retracting the fibrin network. Clot retraction can be inhibited by interruption of the fibrin–platelet integrin receptor complex[45] via blocking antibodies[46] or genetic defects in the platelet integrin receptor

Table II
Histological O'Driscoll scores. Median (range)

Eight week repaired trochlear defect sections ($n = 16$)				
	Between drill holes		Over drill holes	
	Untreated	Treated	Untreated	Treated
I Chondrocyte cell morphology (0–4)	1 (1–4)	3.5 (1–4)†	2 (1–4)	4 (2–4)†
II Toluidine Blue stain (0–3)	1 (0–3)	2.5 (1–3)‡	2 (1–3)	3 (1–3)*
III Surface regularity (0–3)	3 (2–3)	3 (3)	3 (2–3)	3 (3)
IV Structural integrity (0–2)	2 (0–2)	2 (1–2)	2 (1–2)	2 (1–2)
V Thickness (0–2)	0 (0–2)	0.5 (0–2)	1 (0–2)	1 (0–2)
VI Bonding with adjacent cartilage (0–2)	0 (0–1)	0 (0–2)	0 (0–2)	0 (0–1)
VII Normal cellularity (0–3)	2 (0–3)	3 (2–3)†	2 (0–3)	3 (2–3)†
VIII No chondrocyte clustering (0–2)	2 (0–2)	2 (0–2)	2 (1–2)	2 (1–2)
IX Free from degeneration in adjacent cartilage (0–3)	2 (2–3)	2 (2–3)	2 (2–3)	2 (2–3)
Total score (maximum = 24)	13 (4–20)	18.5 (14–21)‡	17 (10–21)	19.5 (14–21)*

*$P < 0.05$ compared to untreated; †$P < 0.005$ compared to untreated; ‡$P < 0.0005$ compared to untreated.

(GPIIb, GPIIIa)[45,47], suggesting that chitosan may interfere with fibrin–platelet interactions. Given that chitosan–GP/blood clots solidified after a 5–10 min delay, retracted slightly, and contained thin fibrin-like fibers, it nonetheless appears that the clotting cascade and generation of a fibrin network are part of the structural stabilization of the hybrid chitosan–GP/blood clot.

CHITOSAN–GP/BLOOD CLOTS STIMULATE CHANGES IN THE SUBCHONDRAL BONE PLATE THAT LEAD TO HYALINE CARTILAGE REPAIR

A bilateral rabbit cartilage repair model was developed to study the effect of chitosan–GP/blood implants on cartilage repair following marrow stimulation. After 8 weeks of repair, a similar average amount of repair tissue was formed in control and treated defects although the repair tissue integration and quality were significantly improved by treatment. In this rabbit study, as well as in our previous ovine cartilage repair study[26], chitosan–GP/blood implants elicited a more hyaline and cellular repair cartilage in marrow-stimulated defects compared to marrow stimulation alone. The repair tissue in treated rabbit defects was still somewhat heterogeneous and was not entirely composed of hyaline cartilage, which could be partly related to the early time point studied, and also to the use of trochlear defects which developed significantly less hyaline cartilage repair than condylar defects in sheep[26]. We have found that an 8-week repair period in this particular rabbit model was a minimal yet sufficient time period needed to measure a significant improvement in repair over controls. Longer repair periods in this rabbit model will allow us to characterize repair tissue durability.

The aim of marrow stimulation is to generate access channels for repair cells, including pluripotent bone marrow stromal cells, to migrate into the chondral defect and possibly give rise to chondrocytes and hyaline cartilage matrix. In all drilled defects, hyaline cartilage repair was frequently detected in areas where bone repair or remodeling gave rise to a porous bone plate [Figs. 5(E,F), 6(B), 7(E)], while fibrous or fibrocartilage tissue was principally observed in regions of failed bone repair [Figs. 3(C), 7(B)] and in regions of failed repair tissue–bone integration [Figs. 5(C), 6(G), 7(B), Table II, between holes]. Taken together, these observations are consistent with the notion that chondral precursors can gain access to the defect by regenerating or remodeling bone. The failure of integrated repair tissue to form over large areas of calcified cartilage in this study [Fig. 6(A)], and in other studies[8–10,48,49] could be partly explained by the inability of marrow-derived repair cells to adhere to, and migrate over, large areas of mineralized tissue containing negatively charged GAG. Repair tissue was able to form over debrided bone in controls [Fig. 5(B), 6(G), 7(B)], however, the tissue frequently failed to adhere [Fig. 5(C)], as previously observed after resurfacing procedures in rabbit[6] and human patients[2].

The formation of more integrated and hyaline tissue by chitosan clot implants could be related to several mechanisms. Residual chitosan clot implant adhering to trochlear calcified cartilage and bone[26] could potentially provide an adhesive surface onto which repair tissues growing from the marrow holes could attach. Stimulation by chitosan clots of bone remodeling between the drill holes[39], and remodeling and resorption of the calcified cartilage layer [Figs. 5(A), 6(B)] could give direct access to the defect by marrow cells in the bone plate, including blood microvessel pericyte chondral progenitors[50]. Finally, chitosan clots stimulated cell recruitment and transient subchondral angiogenesis during acute repair[39], which in this study, and also in our ovine model[26], led to the generation of a porous, revascularized subchondral bone plate [Figs. 5(E,F), 6(D,H), 7(E)]. Cartilage repair tissue integrated with a local vascular supply protected by bone could serve to provide progenitors, oxygen and nutrients, or other marrow-derived factors that stimulate chondrogenic proliferation, differentiation, and hyaline matrix production.

Acknowledgments

We would like to thank Caroline Tanguay and Francine Derome for excellent technical assistance. This research was partly funded by the Canadian Arthritis Network, and the Canadian Institutes of Health Research.

References

1. Mankin HJ. The response of articular cartilage to mechanical injury. J Bone Joint Surg Am 1982;64:460–6.
2. Insall JN. Intra-articular surgery for degenerative arthritis of the knee. A report of the work of the late K.H. Pridie. J Bone Joint Surg Br 1967;49:211–28.

3. Johnson LL. Arthroscopic abrasion arthroplasty: a review. Clin Orthop 2001;S306–17.
4. Steadman JR, Rodkey WG, Singleton SB, Briggs KK. Microfracture technique for full-thickness chondral defects: technique and clinical results. Oper Tech Orthop 1997;7:300–4.
5. Meachim G, Roberts C. Repair of the joint surface from subarticular tissue in the rabbit knee. J Anat 1971;109: 317–27.
6. Mitchell N, Shepard N. The resurfacing of adult rabbit articular cartilage by multiple perforations through the subchondral bone. J Bone Joint Surg Am 1976;58: 230–3.
7. Menche DS, Frenkel SR, Blair B, Watnik NF, Toolan BC, Yaghoubian RS, *et al*. A comparison of abrasion burr arthroplasty and subchondral drilling in the treatment of full-thickness cartilage lesions in the rabbit. Arthroscopy 1996;12(3):280–6.
8. Breinan HA, Martin SD, Hsu HP, Spector M. Healing of canine articular cartilage defects treated with microfracture, a type-II collagen matrix, or cultured autologous chondrocytes. J Orthop Res 2000;18:781–9.
9. Shamis LD, Bramlage LR, Gabel AA, Weisbrode S. Effect of subchondral drilling on repair of partial-thickness cartilage defects of third carpal bones in horses. Am J Vet Res 1989;50(2):290–5.
10. Hanie EA, Sullins KE, Powers BE, Nelson PR. Healing of full-thickness cartilage compared with full-thickness cartilage and subchondral bone defects in the equine third carpal bone. Equine Vet J 1992;24:382–6.
11. Knutsen G, Engebretsen L, Ludvigsen TC, Drogset JO, Grontvedt T, Solheim E, *et al*. Autologous chondrocyte implantation compared with microfracture in the knee. A randomized trial. J Bone Joint Surg Am 2004;86-A: 455–64.
12. Wei XC, Messner K. Maturation-dependent durability of spontaneous cartilage repair in rabbit knee joint. J Biomed Mater Res 1999;46(4):539–48.
13. Kim HK, Moran ME, Salter RB. The potential for regeneration of articular cartilage in defects created by chondral shaving and subchondral abrasion. An experimental investigation in rabbits. J Bone Joint Surg Am 1991;73(9):1301–15.
14. Malette WG, Quigley HJ, Gaines RD, Johnson ND, Rainer WG. Chitosan: a new hemostatic. Ann Thorac Surg 1983;36:55–8.
15. Brandenberg G, Leibrock LG, Shuman R, Malette WG, Quigley H. Chitosan: a new topical hemostatic agent for diffuse capillary bleeding in brain tissue. Neurosurgery 1984;15:9–13.
16. Klokkevold PR, Subar P, Fukayama H, Bertolami CN. Effect of chitosan on lingual hemostasis in rabbits with platelet dysfunction induced by epoprostenol. J Oral Maxillofac Surg 1992;50:41–5.
17. Rao SB, Sharma CP. Use of chitosan as a biomaterial: studies on its safety and hemostatic potential. J Biomed Mater Res 1997;34:21–8.
18. Kojima K, Okamoto Y, Miyatake K, Kitamura Y, Minami S. Collagen typing of granulation tissue induced by chitin and chitosan. Carbohydr Polym 1998;37(2):109–13.
19. Minami S, Rakshit SK, Chandrakrachang S, Stevens WF. Management of fracture with chitosan in dogs. Indian Vet J 2000;77:1085–9.
20. Ueno H, Nakamura F, Murakami M, Okumura M, Kadosawa T, Fujinag T. Evaluation effects of chitosan for the extracellular matrix production by fibroblasts and the growth factors production by macrophages. Biomaterials 2001;22:2125–30.
21. Lee KY, Ha WS, Park WH. Blood compatibility and biodegradability of partially N-acylated chitosan derivatives. Biomaterials 1995;16:1211–6.
22. Varum KM, Myhr MM, Hjerde RJ, Smidsrod O. *In vitro* degradation rates of partially N-acetylated chitosans in human serum. Carbohydr Res 1997;299:99–101.
23. Onishi H, Machida Y. Biodegradation and distribution of water-soluble chitosan in mice. Biomaterials 1999; 20(2):175–82.
24. VandeVord PJ, Matthew HW, DeSilva SP, Mayton L, Wu B, Wooley PH. Evaluation of the biocompatibility of a chitosan scaffold in mice. J Biomed Mater Res 2002;59:585–90.
25. de Campos AM, Diebold Y, Carvalho ELS, Sanchez A, Alonso M. Chitosan nanoparticles as new ocular drug delivery systems: in vitro stability, in vivo fate, and cellular toxicity. Pharm Res 2004;21:803–11. ISSN 0724-8741.
26. Hoemann CD, Hurtig MB, Rossomacha E, Sun J, Chevrier A, Shive MS, *et al*. Chitosan–glycerol phosphate/blood implants improve hyaline cartilage repair in ovine microfracture defects. J Bone Joint Surg Am 2005;87(12):2671–86.
27. Chenite A, Chaput C, Wang D, Combes C, Buschmann MD, Hoemann CD, *et al*. Novel injectable neutral solutions of chitosan form biodegradable gels *in-situ*. Biomaterials 2000;21:2155–61.
28. Hoemann CD, Sun J, Legare A, McKee MD, Buschmann MD. Tissue engineering of cartilage using an injectable and adhesive chitosan-based cell delivery vehicle. Osteoarthritis Cartilage 2005;13: 318–29.
29. Filion D, Lavertu M, Buschmann MD. Titration and phase-separation of chitosan solutions related to thermosensitive chitosan/glycerol-phosphate systems (Submitted for publication).
30. Shapiro F, Koide S, Glimcher MJ. Cell origin and differentiation in the repair of full-thickness defects of articular cartilage. J Bone Joint Surg Am 1993;75A(4): 532–53.
31. O'Driscoll SW, Keeley FW, Salter RB. Durability of regenerated articular cartilage produced by free autogenous periosteal grafts in major full-thickness defects in joint surfaces under the influence of continuous passive motion. A follow-up report at one year. J Bone Joint Surg Am 1988;70(4):595–606.
32. Rao AK. Acquired qualitative platelet defects. In: Colman RW, Hirsh J, Marder VJ, Clowes AW, George JN, Eds. Hemostasis and Thrombosis. 4th edn. New York: Lippincott Williams & Wilkins 2001: 910.
33. Kase F, Pospisil J. Comparison of the blood clotting mechanisms in man and some common laboratory animals. Acta Univ Carol Med Monogr 1987;119:11–22.
34. Owen CA Jr. Historical account of tests of hemostasis. Am J Clin Pathol 1990;93:S3–8.
35. Beutler E. Osmotic fragility. In: Beutler E, Lichtman MA, Coller BS, Kipps TJ, Seligsohn U, Eds. Williams Hematology. 6th edn. New York: McGraw-Hill 2001: L46–L47.
36. Rossomacha E, Hoemann CD, Shive MS. Simple methods for staining chitosan in biotechnological applications. J Histotechnol 2004;27:31–6.
37. Chevrier A, Rossomacha E, Buschmann MD, Hoemann CD. Optimization of histoprocessing

methods to detect glycosaminoglycan, collagen type I and collagen type II in decalcified rabbit osteochondral sections. J Histotechnol 2005;28:165–75.
38. Griffiths G. Quantitative aspects of immunocytochemistry. Chapter 11, Fine Structure Immunocytochemistry. New York: Springer-Verlag 1993; 371–441.
39. Chevrier A, Hoemann CD, Sun J, Buschmann MD. Chitosan–glycerol phosphate/blood implants increase cell recruitment, transient vascularization and subchondral bone remodeling in drilled cartilage defects (Submitted for publication).
40. Eriksen EF, Axelrod DW, Melsen F. Bone macroanatomy and microanatomy, Bone Histomorphometry. New York: Raven Press 1994; Chapter 2: 3–12.
41. Okamoto Y, Yano R, Miyatake K, Tomohiro I, Shigemasa Y, Minami S. Effects of chitin and chitosan on blood coagulation. Carbohydr Polym 2003;53: 337–42.
42. Hirano S, Noishiki Y. The blood compatibility of chitosan and N-acylchitosans. J Biomed Mater Res 1985; 19:413–7.
43. Olsen R, Schwartzmiller D, Weppner W, Winandy R. Biomedical applications of chitin and its derivatives. In: Proceedings of the Fourth International Conference on Chitin and Chitosan. Trondheim, Norway. 1989;4: 813–28
44. Chou TC, Fu E, Wu CJ, Yeh JH. Chitosan enhances platelet adhesion and aggregation. Biochem Biophys Res Commun 2003;302:480–3.
45. Cohen I, Gerrard JM, White JG. Ultrastructure of clots during isometric contraction. J Cell Biol 1982;93:775–87.
46. Coller BS, Peerschke EI, Scudder LE, Sullivan CA. A murine monoclonal antibody that blocks fibrinogen binding to normal platelets also inhibits fibrinogen interactions with chymotrypsin-treated platelets. Blood 1984;64:59–63.
47. Nurden AT, George JN. Inherited abnormalities of the platelet membrane: Glanzmann thrombasthenia, Bernard-Soulier syndrome, and other disorders. In: Colman RW, Hirsh J, Marder VJ, Clowes AW, George JN, Eds. Hemostasis and Thrombosis. 4th edn. New York: Lippincott Williams & Wilkins 2001:921–2.
48. Nehrer S, Breinan HA, Ramappa A, Hsu HP, Minas T, Shortkroff S, *et al*. Chondrocyte-seeded collagen matrices implanted in a chondral defect in a canine model. Biomaterials 1998;19(24):2313–28.
49. Hurtig M, Fretz PB, Doige CE, Schnurr DL. Effects of lesion size and location on equine articular cartilage repair. Can J Vet Res 1988;52:137–46.
50. Farrington-Rock C, Crofts NJ, Doherty MJ, Ashton BA, Griffin-Jones C, Canfield AE. Chondrogenic and adipogenic potential of microvascular pericytes. Circulation 2004;110:2226–32.